

Direct observation of the superconducting energy gap developing in the conductivity spectra of niobium

A. V. Pronin,* M. Dressel, A. Pimenov, and A. Loidl

Experimentalphysik V, Universität Augsburg, Universitätsstrasse 2, D-86135 Augsburg, Germany

I. V. Roshchin and L. H. Greene

Department of Physics, University of Illinois at Urbana-Champaign, Urbana, Illinois 61801

(Received 23 October 1997)

The electrodynamic response of Nb in the frequency range above and below the energy gap 2Δ is studied in the normal and in the superconducting state. A coherent source interferometer is utilized in the spectral range between 5 and 30 cm^{-1} to investigate the amplitude and the phase of the transmission through niobium films that allows the direct determination of both components of the complex conductivity. The optical conductivity up to 300 cm^{-1} is evaluated using infrared reflection measurements. Below the 8.31-K superconducting transition temperature of the 150-Å-thick film, the superconducting energy gap is observed to increase as the temperature decreases. The overall frequency dependence of the conductivity can be described using the BCS formalism and assuming finite scattering effects; however, at low temperatures we find deviations from the predicted behavior in the spectral range below the energy gap. Estimations of the gap at zero temperature $2\Delta(0) = 24 \text{ cm}^{-1}$ or $4.1k_B T_c$ deviate from the weak-coupling BCS limit. [S0163-1829(98)03421-3]

I. INTRODUCTION

Studies of the electrodynamic properties of superconductors in the frequency range between microwaves and far infrared have played a critical role in the confirmation of the Bardeen-Cooper-Schrieffer (BCS) theory of superconductivity.¹ Some of the important steps were measurements of the frequency- and temperature-dependent microwave absorption in Al,² the absorption of thin films of Pb, Sn, and In,³ and the transmission through thin Sn and Pb films,⁴ which helped to establish the existence of the superconducting energy gap. For most of the conventional superconductors, the energy gap is expected to be in the millimeter and submillimeter range, which allows the study of the excitation spectrum of the quasiparticles. However, most of the experiments on the electrodynamic properties of superconductors measure only the surface resistance or the transmission, and thus do not allow the direct determination of the frequency dependence of both components of the conductivity. One of the few exceptions is the classical paper of Palmer and Tinkham⁵ in which, by measuring simultaneously both the reflection and transmission through thin Pb films, the optical conductivity was obtained above and slightly below the superconducting energy gap. These also gave evidence for strong-coupling effects.

Despite numerous studies, for Nb the influence of strong coupling is not as clear as it is for Pb or Hg (for a recent review, see Ref. 6). As early as 1960, Richards and Tinkham⁷ inferred the energy gap of Nb by far-infrared (FIR) absorption measurements and obtained $2\Delta = 2.8k_B T_c$. Tunneling experiments^{6,8} yield $2\Delta/k_B T_c = 3.6\text{--}3.96$ and provide evidence for deviations from the BCS predictions. The analysis of the ultrasonic attenuation leads to even higher gap values.⁹ Electrodynamic measurements in the time domain conducted at $T = 4.7$ K allowed the determination of the energy gap in Nb from the onset of

absorption;¹⁰ the conductivity spectra above the superconducting energy gap was described by the BCS theory using the Mattis-Bardeen formulas.¹¹ The reports on experimental results of the surface impedance in the microwave range of frequency are contradictory. Anlage *et al.*¹² describe their data by the BCS theory but obtain a rather large ratio of $2\Delta/k_B T_c = 4.0\text{--}4.2$. A good agreement with the weak-coupling predictions was obtained from measurement of the temperature-dependent surface impedance by Klein *et al.*,¹³ for their data strong-coupling correction led to only a minor improvement of the fit. Marsiglio *et al.*¹⁴ were not able to describe their results obtained by a similar technique at a somewhat lower frequency either by the simple BCS model or by performing calculations according to the Eliashberg theory with the behavior of $F(\omega)\alpha^2(\omega)$ evaluated from tunneling measurements.

We present here the direct observation of the temperature-dependent energy gap of superconducting niobium films as measured in the complex conductivity spectra in the 5–30 cm^{-1} frequency range. In combination with our FIR reflectivity measurements, this enables us to analyze the temperature dependence and the spectral shape of the optical conductivity in a wide range of frequency above and below the superconducting gap.

II. EXPERIMENTAL DETAILS

The high-quality $10 \times 10\text{-mm}^2$ niobium film is grown by planar magnetron sputter deposition on a plane-parallel $d_s = 0.45$ mm thick sapphire substrate oriented in the (1102) plane. An *in situ* bake at 490–500 °C is performed during a 50-h pumpdown before the niobium deposition to clean the sapphire surface of water and hydrocarbons. After a base pressure lower than 8×10^{-9} Torr was reached, high-purity Ar is leaked into the system to a pressure of 7.0×10^{-3} Torr and the Nb film is deposited at a rate of

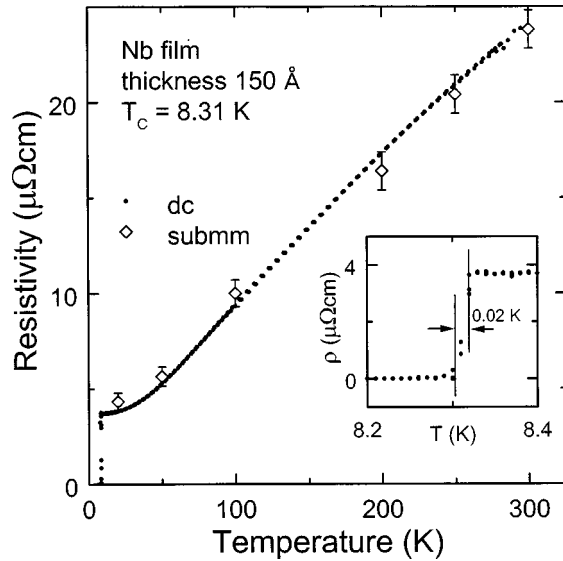


FIG. 1. Temperature dependence of the dc resistivity and the inverse conductivity $1/\sigma_1$ obtained in the submillimeter wave range of a Nb film with a thickness of 150 Å on a 0.45-mm sapphire substrate. The inset shows an enlargement of the superconducting transition at $T_c = 8.31$ K.

8 Å/s. The film thickness is 150 Å. The inset to Fig. 1 shows the resistivity versus temperature taken in the standard four-probe geometry. The superconducting transition at $T_c = 8.31$ K is sharp, exhibiting a width of 0.02 K, as determined from the 90% and 10% values of the resistivity drop. The slightly reduced value of the transition temperature from the bulk value of 9.2 K is commonly seen in high-quality thin Nb films.¹⁵ The temperature-dependent dc resistivity (Fig. 1) exhibits typical Bloch-Grüneisen behavior: It is linear at higher temperatures and approaches a constant value below about 30 K. The residual resistivity ratio, $\rho_{300\text{ K}}/\rho_{10\text{ K}}$, is equal to 6.5. In the metallic state, the inverse conductivity $1/\sigma_1$ obtained in the submillimeter wave range of frequency is in excellent agreement with the dc results.

The measurements in the millimeter and submillimeter wave range of frequency are performed using a coherent-source spectrometer¹⁶ sketched in Fig. 2. Four backward wave oscillators operating in partially overlapping frequency

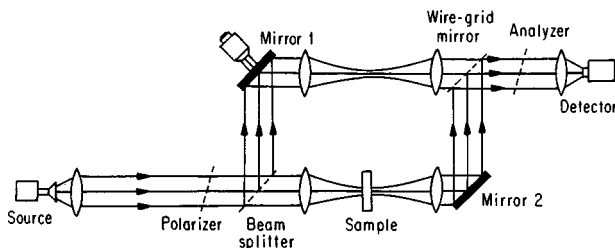


FIG. 2. Setup of the coherent source spectrometer that can be used in the frequency range from 2 to 50 cm^{-1} . The monochromatic radiation is provided by tunable backward wave oscillators; polyethylene lenses focus the beam; wire grids are used as polarizers and beam splitters; the radiation is detected by a Golay cell or a He-cooled bolometer. The sample placed in a cryostat is positioned in one arm of the Mach-Zehnder interferometer; the second path can be adjusted in its optical path length to measure the phase difference.

ranges were employed as monochromatic and continuously tunable sources covering the range from 5 to 30 cm^{-1} . The arrangement of a Mach-Zehnder interferometer allows for measuring both the intensity and the phase shift of the radiation transmitted through the sample, i.e., the niobium film on the substrate. Such transmission measurements of thin films have proven to be a powerful method for studying the electrodynamic properties of a wide variety of highly conductive thin-film materials.^{17,18}

In addition, temperature-dependent polarized reflectivity measurements are performed in the FIR (20–500 cm^{-1}) using a Bruker IFS 113v Fourier-transform interferometer. In order to increase the sensitivity of the reflection measurement we employ the resonant technique developed in Ref. 19. The substrate orientation with the film faced to the back allows us to use the sapphire substrate as a Fabry-Pérot resonator. The change in the reflection amplitude and frequency of the interference fringes upon cooling through the superconducting transition allows for evaluation of both components of the complex conductivity in the normal and superconducting state without performing a Kramers-Kronig analysis.¹⁹ The experiments with both spectrometers are performed in the 4.5–300-K temperature range in a He-bath cryostat, with the sample surrounded by He-exchange gas.

III. RESULTS AND ANALYSIS

Examples of the raw transmission and phase-shift spectra, taken both above and below the superconducting critical temperature ($T_c = 8.31$ K), are displayed in Fig. 3. In the transmission spectra, the well-developed fringes result from the multireflection of the light within the sapphire substrate, which behaves as a nonsymmetric Fabry-Pérot resonator. The period of the oscillations is mainly governed by the refractive index n_s and the thickness d_s of the substrate. Due to the low losses of sapphire in this spectral range, the level of the transmission is dominated by the transparency of the niobium film, which is determined by the real part of the conductivity σ_1 and, in particular, in the superconducting state, by the imaginary part σ_2 . The overall frequency dependence (i.e., the slope) of the phase-shift spectrum is controlled by the substrate parameters, while the shape of phase oscillations mainly depends on the film properties.²⁰

At a given temperature $T > T_c$, the amplitude of the interference fringes is constant within our frequency range. When the temperature decreases (but remaining in the metallic state), the periodicity of the transmission spectra does not change, but the transmission magnitude is reduced with temperature [Fig. 3(a), inset] as a result of the increasing film conductivity. Below T_c the spectrum alters considerably as can be seen in Fig. 3: at low frequencies the transmission diminishes, while above approximately 20 cm^{-1} it increases with respect to the normal-state values. This indicates a strongly frequency-dependent complex conductivity. The magnitude of the phase shift remains almost constant in the normal state, but rapidly drops below T_c , e.g., the reduction at 5.7 cm^{-1} is more than 1 rad [inset of Fig. 3(b)].

The evaluation of the electrodynamic parameters of the Nb film uses the general Fresnel formulas²¹ for a two-layer system (i.e., the film on the substrate) by simultaneous analysis of the observed transmission and phase spectra without

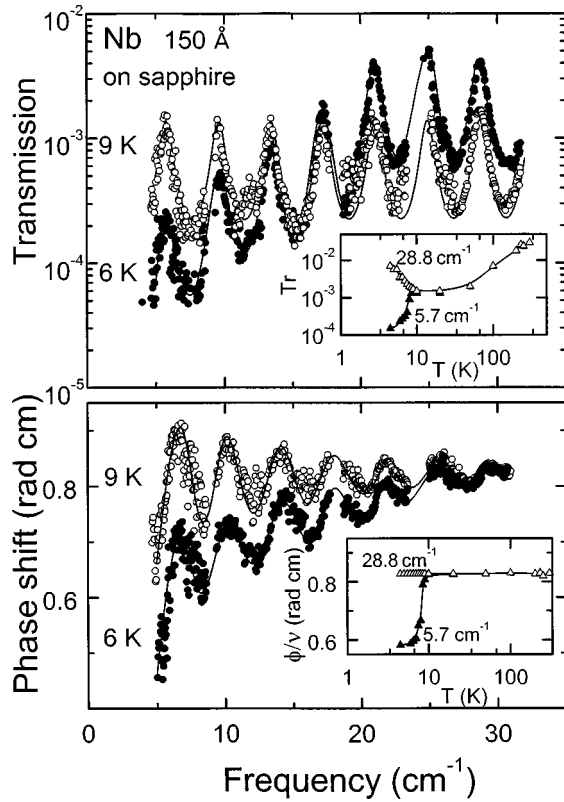


FIG. 3. Original transmission $\text{Tr}(\nu)$ and phase shift $\varphi(\nu)$ spectra of the Nb film on the Al_2O_3 substrate. The phase shift is divided by the frequency for the better perception. The dots represent the measured values, the lines for 9 K are the fit with the Drude model. In the insets the temperature dependence of Tr and φ is displayed for two particular frequencies corresponding to the first and last transmission maxima in our spectral range.

assuming any particular model and without referring to the Kramers-Kronig relations. Since the description of the interference pattern is most sensitive to the optical properties of the film near the transmission maxima, only data at these frequencies are evaluated further. The optical parameters of the substrate are determined by separately measuring the temperature-dependent transmission and the phase shift of a bare sapphire plate of the same orientation. At low temperatures we obtain approximately $n_s \approx 3.0$ and $k_s \approx 0.001$ with just a slight variation with frequency in the millimeter-submillimeter wave range. A detailed description of the measurement technique, the analysis of the spectra, and the evaluation of the conductivity will be given elsewhere.²⁰ The FIR data are analyzed by fitting the observed interference fringes with Fresnel's formulas, again using the measured values of the optical parameters of sapphire in the relevant orientation and temperature. Below 80 cm^{-1} a reliable analysis of the data is not possible because the signal intensity is too low. Due to the strong absorption by phonons of the sapphire, the evaluation of the film properties is limited to frequencies below 300 cm^{-1} .

In the normal state the electrodynamic properties of the Nb film can be consistently interpreted in terms of a metallic conductivity. The normal-state properties in the $5\text{--}30\text{-cm}^{-1}$ spectral range show that both the real and imaginary parts of the dynamical conductivity $\sigma_1(\nu)$ and $\sigma_2(\nu)$ are frequency independent; the real part is equal to the static value σ_{dc} and

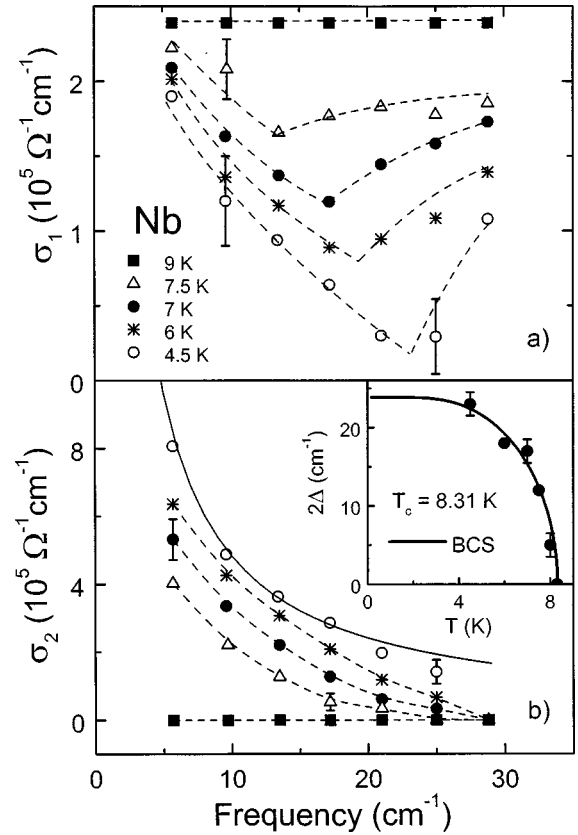


FIG. 4. (a) Real part of conductivity of Nb vs frequency for $T = 9 \text{ K}$ and several temperatures below $T_c = 8.3 \text{ K}$ as indicated. The dashed lines are guides to the eye. (b) Imaginary part of conductivity as a function of frequency. The dashed lines are guides to the eye. The solid line represents the $1/\nu$ behavior predicted for low temperatures. The inset shows the temperature dependence of the energy gap $2\Delta(T)$ evaluated from the frequency and temperature dependence of the optical conductivity. The line corresponds to the BCS prediction with $T_c = 8.31 \text{ K}$ and $2\Delta(0)/k_B T_c = 4.1$.

the imaginary part of the conductivity σ_2 is basically zero within the experimental accuracy. As the temperature is lowered from room temperature down to about $T = 30 \text{ K}$, the real part of the conductivity increases and becomes approximately constant at $T < 30 \text{ K}$ in a good agreement with dc measurements (Fig. 1). This frequency behavior of the complex conductivity is in accordance with the Drude model in the low-frequency limit $\nu \ll \gamma$ (Hagen-Rubens regime), where ν is the frequency and $\gamma = 1/(2\pi\tau)$ is the relaxation rate. From our FIR data we clearly see the roll-off of the conductivity and obtain $\gamma \approx 150 \text{ cm}^{-1}$ at low temperatures as shown in Fig. 5(a).

In Fig. 4 the real and imaginary parts of the conductivity of Nb, as derived from transmission and phase-shift spectra, are plotted for temperatures below 10 K . While being constant in the normal state, the conductivity $\sigma_1(\nu)$ exhibits a strong frequency dependence at temperatures below T_c . We attribute the minimum of the optical conductivity to the energy gap $2\Delta(T)$ of the superconducting state.^{11,22} In agreement with predictions^{1,22} of the temperature dependence of the energy gap $2\Delta(T)$, the minimum of the $\sigma_1(\nu)$ becomes more pronounced and shifts to higher frequencies as the temperature decreases. The temperature dependence of the gap, estimated from the experimental data (Fig. 4, inset), can be

TABLE I. Measured and evaluated electrodynamic properties of niobium. The London penetration depth $\lambda_L(0)$ is calculated from $\lambda(0)$ according to Ref. 24 using the presented values of the coherence length ξ_0 and the mean free path l . The plasma frequency ω_p is evaluated from the London penetration depth.

Transition temperature T_c (K)	Energy gap		Coherence length $\xi_0 = \hbar v_F / \pi \Delta(0)$ (Å)	Mean free path $l(T=9\text{ K})$ (Å)	$\pi \xi_0 / l$	Observed penetration depth $\lambda(0)$ (Å)	London penetration depth $\lambda_L(0)$ (Å)	Plasma frequency $\hbar \omega_p$ (eV)
	$2\Delta(0)$ (cm^{-1})	$2\Delta(0)/k_B T_c$						
8.31	24	4.1	390	90	13	900	350	5.8

well described by the mean-field theory. The fit by the BCS curve yields $2\Delta(0) = 24 \pm 1.5 \text{ cm}^{-1}$ and $2\Delta(0)/k_B T_c = 4.1 \pm 0.3$. The latter value deviates from the weak-coupling BCS limit [$2\Delta(0)/k_B T_c = 3.53$] and indicates intermediate or strong type of electron-phonon coupling in niobium. Our result is in accordance with estimations based on ultrasonic attenuation,⁹ optical measurements,^{10,12} and tunneling measurements^{6,8} of the gap parameter.

The frequency dependence of the imaginary part of the conductivity $\sigma_2(\nu)$ is displayed in Fig. 4(b) for several temperatures $T < T_c$. When the gap energy is much higher than the frequency of the radiation used, i.e., at low frequencies and at low temperatures, the imaginary part $\sigma_2(\nu)$ is proportional to $1/\nu$. According to the Kramers-Kronig relation, this corresponds to the δ function of the dc conductivity $\sigma_1(\nu=0)$.²² At higher frequencies and higher temperatures we observe deviations from this behavior due to the influence of the proximity of the energy gap in the conductivity spectra.

IV. DISCUSSION

From our measurements we can determine some important electrodynamic parameters of niobium such as the penetration depth λ , the plasma frequency ω_p , and the mean free path l ; the values are presented in Table I. Using the standard formula²³ for the penetration depth $\lambda = c/(2\pi k\nu)$, with the extinction coefficient k calculated from the real and imaginary part of the conductivity, we find $\lambda(T=0) = 900 \pm 50 \text{ Å}$ by extrapolating to zero temperature. The inset of Fig. 5 presents the temperature dependence of $\lambda^2(0)/\lambda^2(T)$ at lowest measuring frequency in comparison with the BCS calculations. The figure reveals deviations from the weak-coupling BCS limit in the way expected for strong-coupling effects.²²

In the London limit the penetration depth is related to the plasma frequency by the simple equation $\lambda_L(T=0) = c/\omega_p$. However, according to our results on $\sigma_1(\nu)$ shown in Fig. 4(a), the scattering rate in Nb is larger than the energy gap by approximately a factor of 2 which means that the condition of the London limit is not realized and that we cannot use this simple relation for the determination of the plasma frequency. Instead we have to take into account the influence of the finite mean free path and employ the general relation between the actual penetration depth λ and its London limit λ_L given in Ref. 24 [the coherence length can be found by use of a standard expression $\xi_0 = \hbar v_F / \pi \Delta(T=0) = 390 \text{ Å}$ utilizing our obtained value of the gap $2\Delta(0) = 24 \text{ cm}^{-1}$ and the mean-field value of the Fermi velocity $v_F = 0.3 \times 10^8 \text{ cm/s}$ from Ref. 25]. Using this relation to-

gether with the standard Drude expression $2\sigma_{dc}\gamma = v_p^2$ yields $\gamma = 150 \text{ cm}^{-1}$ or $l = v_F \tau = 90 \text{ Å}$ and $\hbar \omega_p = 5.8 \text{ eV}$ (corresponding to $\nu_p = \omega_p/2\pi = 7.2 \times 10^4 \text{ cm}^{-1}$), suggesting the value of the scattering rate in the superconducting state equals that at temperatures just above T_c . All these values are in good agreement with literature data obtained by different experimental methods.^{7,25,26}

In Fig. 5 the experimentally obtained spectra of $\sigma_1(\nu)$ and $\sigma_2(\nu)$ are compared with the behavior as calculated using the simple Mattis-Bardeen equations but including a finite scattering rate.^{11,22,27} Parameters of these calculations [$2\Delta(0) = 24 \text{ cm}^{-1}$ and $\pi \xi_0 / l = 13$] were taken only from the millimeter-submillimeter measurements. We found the cal-

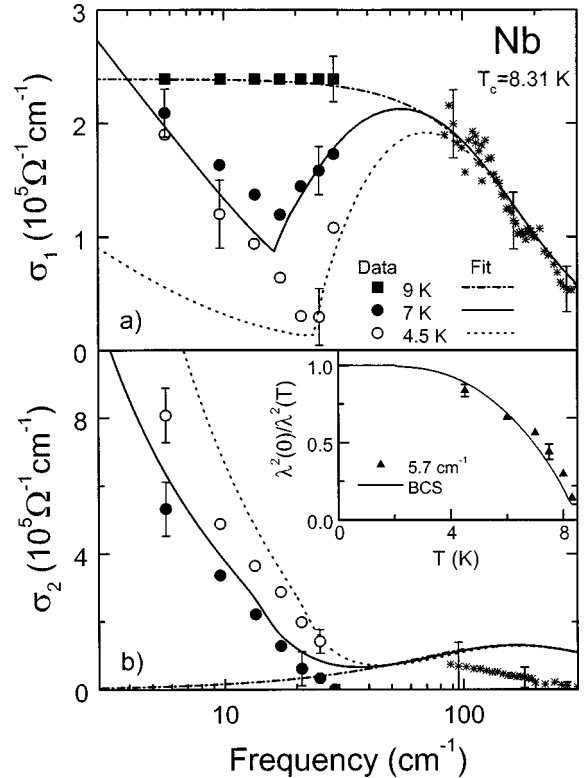


FIG. 5. Frequency dependence of the (a) real and (b) imaginary parts of the conductivity at 4.5 and 7 K compared to the predictions of the BCS weak-coupling limit by using the formulas of Mattis and Bardeen with a finite scattering time $\tau \approx 3 \times 10^7 \text{ s}$ (Refs. 22 and 26). Also shown is the normal-state behavior at $T = 9 \text{ K}$ fitted by the Drude model. The FIR data (stars) show no temperature dependence below 10 K. In this spectral range, the imaginary part of the conductivity $\sigma_2(\nu)$ has large error bars. The inset shows the temperature dependence of the penetration depth $\lambda(T)$ compared with the predicted behavior.

culated spectra of $\sigma_1(\nu)$ and $\sigma_2(\nu)$ in very good agreement with FIR conductivity obtained from the reflection experiments. The FIR data show no changes for temperatures between 4.5 and 9 K, confirming that γ is temperature independent below 10 K. For $T=9$ K the optical conductivity $\sigma_1(\nu)$ is well described by a Drude behavior with $\sigma_{dc}=2.4 \times 10^5 (\Omega \text{ cm})^{-1}$ and a scattering rate of $\gamma \approx 150 \text{ cm}^{-1}$, which is exactly the value obtained from the analysis of the penetration depth in the superconducting state discussed in the previous paragraph. At $T=7$ K the data are in good agreement with the evaluations done in the framework of the BCS theory. As the temperature is lowered, we observe a considerably higher conductivity in the frequency range below the superconducting energy gap than predicted. Our findings agree with the measurements of the surface impedance at $\nu=0.6 \text{ cm}^{-1}$ by Marsiglio *et al.*¹⁴ who found $\sigma_1/\sigma_n \approx 1.8$ which is about a factor of 3 higher than the BCS value at $T/T_c=0.54$. Both results are not compatible with the surface-impedance measurements performed at 2 cm^{-1} .¹³ Our values of $\sigma_2(\nu)$ are about 40% smaller than the calculated ones. A similar observation was made by Nuss *et al.*¹⁰ and related to strong-coupling effects. It is difficult to evaluate $\sigma_2(\nu)$ from the reflectivity experiments in the FIR and the data presented in Fig. 5(b) represent only an estimate with large error bars.

In agreement with the findings of Marsiglio *et al.*,¹⁴ our data cannot be described by the Eliashberg theory using $F(\omega)\alpha^2(\omega)$ obtained from tunneling measurements. The frequency and temperature dependence of the conductivity below the superconducting energy gap may provide important information about the electron-phonon spectral function and the inelastic scattering rate.¹⁴ An anisotropy of the supercon-

ducting gap may also lead to low-frequency behavior similar to the one observed. We cannot completely rule out that an increased absorption below the superconducting transition temperature may also be caused by grain boundaries; in addition, finite-size effects have to be considered in films of a thickness comparable to the mean free path.

V. CONCLUSION

We have performed measurements of the optical transmission and phase shift of Nb films and discuss the frequency and temperature dependence of the real and the imaginary parts of the conductivity in the range above and below the superconducting energy gap 2Δ . From the minimum of absorption in the $\sigma_1(\nu)$ spectra we evaluate the temperature dependence of the gap parameter and find that $2\Delta(0)=24 \text{ cm}^{-1}$, corresponding to $2\Delta(0)/k_B T_c=4.1$, which points in the direction of strong-coupling electron-phonon interaction in niobium. From the measured complex conductivity spectra we estimate the plasma frequency and the scattering rate; these parameters agree well with FIR reflectivity measurements and with the literature data.

ACKNOWLEDGMENTS

We thank G. Knebel for performing the dc measurement. The work at Augsburg was supported by the BMBF under Contract No. EKM 13N6917. The German-Russian collaboration was supported by the Deutsche Forschungsgemeinschaft and the Russian Foundation for Basic Research. The film preparation at Urbana was supported by the Department of Energy through the Materials Research Laboratory under Grant No. DE-FG02-91-ER45439.

*Permanent address: Institute of General Physics, Russian Academy of Sciences, 117942 Moscow, Russia.

¹J. Bardeen, L. N. Cooper, and J. R. Schrieffer, *Phys. Rev.* **108**, 1175 (1957).

²M. A. Biondi and M. P. Garfunkel, *Phys. Rev.* **116**, 853 (1959).

³D. M. Ginsberg and M. Tinkham, *Phys. Rev.* **118**, 990 (1960).

⁴R. E. Glover and M. Tinkham, *Phys. Rev.* **108**, 243 (1957).

⁵L. H. Palmer and M. Tinkham, *Phys. Rev.* **165**, 588 (1968).

⁶J. P. Carbotte, *Rev. Mod. Phys.* **62**, 1027 (1990), and references therein.

⁷P. L. Richards and M. Tinkham, *Phys. Rev.* **119**, 575 (1960).

⁸R. Meservey and B. B. Schwartz, in *Superconductivity*, edited by R. D. Parks (Dekker, New York, 1969), Vol. I, p. 117, and references therein.

⁹F. Carsey, R. Kagiwada, M. Levy, and K. Maki, *Phys. Rev. B* **4**, 854 (1971).

¹⁰M. C. Nuss, K. W. Goossen, J. P. Gordon, P. M. Mankiewich, and M. L. O'Malley, *J. Appl. Phys.* **70**, 2238 (1991).

¹¹D. C. Mattis and J. Bardeen, *Phys. Rev.* **111**, 412 (1958).

¹²S. M. Anlage, D.-H. Wu, J. Mao, S. N. Mao, X. X. Xi, T. Venkatesan, J. L. Peng, and R. L. Greene, *Phys. Rev. B* **50**, 523 (1994).

¹³O. Klein, E. J. Nicol, K. Holczer, and G. Grüner, *Phys. Rev. B* **50**, 6307 (1994).

¹⁴F. Marsiglio, J. P. Carbotte, R. Akis, D. Achkir, and M. Poirier, *Phys. Rev. B* **50**, 7203 (1994).

¹⁵L. H. Greene, J. F. Dorsten, I. V. Roshchin, A. C. Abeyta, T. A.

Tanzer, G. Kuchler, W. L. Feldmann, and P. W. Bohn, *Czech. J. Phys.* **46**, Suppl. 6, 3115 (1996).

¹⁶A. A. Volkov, Yu. G. Goncharov, G. V. Kozlov, S. P. Lebedev, and A. M. Prokhorov, *Infrared Phys.* **25**, 369 (1985).

¹⁷B. P. Gorshunov, I. V. Fedorov, G. V. Kozlov, A. A. Volkov, and A. D. Semenov, *Solid State Commun.* **87**, 17 (1993).

¹⁸See, for example, A. V. Pronin, B. P. Gorshunov, A. A. Volkov, G. V. Kozlov, N. P. Shabanova, S. I. Krasnosvobodtsev, and E. V. Pechen Zh. Eksp. Teor. Fiz. **109**, 1465 (1996) [*JETP* **82**, 790 (1996)]; B. P. Gorshunov, A. V. Pronin, A. A. Volkov, H. S. Somal, D. van der Marel, B. J. Feenstra, Y. Jaccard, and J.-P. Locquet, *Physica B* **244**, 15 (1998); M. Dressel, B. P. Gorshunov, A. V. Pronin, A. A. Mukhin, F. Mayr, A. Seeger, P. Lunkenheimer, A. Loidl, M. Jourdan, M. Huth, and H. Adrian, *ibid.* **244**, 125 (1998)

¹⁹K. Kornelsen, M. Dressel, J. E. Eldridge, M. L. Brett, and K. L. Westra, *Phys. Rev. B* **44**, 11 882 (1991); A. Schwartz, M. Dressel, A. Blank, T. Csiba, G. Grüner, A. A. Volkov, B. P. Gorshunov, and G. V. Kozlov, *Rev. Sci. Instrum.* **66**, 2943 (1995).

²⁰B. P. Gorshunov, A. V. Pronin, A. A. Volkov, and M. Dressel (unpublished).

²¹M. Born and E. Wolf, *Principles of Optics*, 4th ed. (Pergamon, Oxford, 1980).

²²G. Rickayzen, *Theory of Superconductivity* (Interscience, New York 1966); M. Tinkham, *Introduction to Superconductivity*, 2nd ed. (McGraw-Hill, New York, 1996).

- ²³L. D. Landau, E. M. Lifshitz, and L. P. Pitaevskii, *Electrodynamics of Continuous Media*, 2nd ed. (Butterworth-Heinemann, Oxford, 1984).
- ²⁴P. B. Miller, Phys. Rev. **113**, 1209 (1959).
- ²⁵See, for example, C. Kittel, *Introduction to Solid State Physics*, 6th ed. (Wiley, New York, 1986); H. W. Weber, E. Seidl, C. Laa, E. Schachinger, M. Prohammer, A. Junod, and D. Eckert, Phys. Rev. B **44**, 7585 (1991); L. F. Mattheiss, Phys. Rev. B **1**, 373 (1970).
- ²⁶R. Blaschke and R. Blocksdorf, Z. Phys. B **49**, 99 (1982).
- ²⁷J.-J. Chang and D. J. Scalapino, Phys. Rev. B **40**, 4299 (1989).